Journal of Solid State Chemistry 183 (2010) 707–711

Contents lists available at ScienceDirect

Journal of Solid State Chemistry

journal homepage: www.elsevier.com/locate/jssc

Magnetic order and heavy fermion behavior in $CePd_{1+x}Al_{6-x}$: Synthesis, structure, and physical properties

Paul H. Tobash [a,b,*], Filip Ronning [a], J.D. Thompson [a], Svilen Bobev [b], Eric D. Bauer [a]

[a] Materials Physics and Application Division, MPA-10, Los Alamos National Laboratory, Los Alamos, NM 87545, USA
[b] Department of Chemistry and Biochemistry, University of Delaware, Newark, DE 19716, USA

ARTICLE INFO

Article history:
Received 10 August 2009
Received in revised form
7 December 2009
Accepted 12 December 2009
Available online 4 January 2010

Keywords:
Crystal structure
Flux growth
Magnetism
Heavy fermion
Specific heat

ABSTRACT

The physical properties including magnetic susceptibility, specific heat, and electrical resistivity of single crystals are reported for the compound $CePd_{1+x}Al_{6-x}$ (x=0.5) which crystallizes in the tetragonal $SrAu_2Ga_5$-type structure (space group $P4/mmm$). The compound was grown from an excess of molten Al flux from the respective elements and the crystal structure was established from single-crystal X-ray diffraction. Anomalies in the low temperature specific heat $C_p(T)$ and electrical resistivity $\rho(T)$ show that the compound undergoes ferromagnetic order at T_C=2.8 K. In the ordered state, $CePd_{1.5}Al_{5.5}$ displays heavy fermion behavior with a Sommerfeld coefficient of ca. 500 mJ/mol-K^2.

Published by Elsevier Inc.

1. Introduction

Many Ce-containing compounds in which the local magnetic moments of Ce hybridize strongly with the conduction electrons at low temperature exhibit remarkable physical properties such as heavy fermion (HF) behavior [1], often with a tendency towards an unconventional superconducting state or magnetic instability [2–6], intermediate valence behavior [7,8], or Kondo insulating behavior [9]. Also of remarkable nature concerns the crystal chemistry for the way in which these compounds are constructed from simpler building block moieties, thereby providing hints for the structure–property relationships responsible for the observed physical properties. Since the discovery of pressured-induced superconductivity in $CeRhIn_5$ [10], a number of isostructural analogs containing transition metals from the same periodic group, i.e. Co and Ir have been synthesized [11,12]. A few other compounds described with the formula Ce_2MIn_8 (M=Co, Rh, Ir) have also been isolated and found to be structurally related [12–14]. Both compounds can be described with the generalized formula $Ce_nM_mIn_{3n+2m}$ where m is the number of $CeIn_3$ slabs and n is the number of MIn_2 slabs. Noteworthy, an essential ingredient for superconductivity in the '115' family of compounds has been suggested to arise from the quasi-two-dimensional $CeIn_3$ layers [10].

The similar crystal chemistry present in the '115' compounds can be extended to three other recently reported compounds, $CePdGa_6$ [15], Ce_2PdGa_{12} [16], and Ce_2PdIn_8 [17]. The alternate layering in the structures of $CePdGa_6$ [15] and Ce_2PdGa_{12} [16] has been suggested to lead to the different properties in both compounds due to the Pd deficiency in the latter [16]. More recently, the coexistence of an antiferromagnetic and superconducting state was discovered in Ce_2PdIn_8 [17] further exemplifying the intimate relationship between both phenomena.

Our motivation in this system was sparked by attempting to extend the family of '115' isostructural analogs to the later transition metals of Ni, Pd and Pt through the incorporation of the smaller Al. These attempts turned out to be unsuccessful and instead led to a new compound described with the formula $CePd_{1+x}Al_{6-x}$ (where x=0.5) which crystallizes with the tetragonal $SrAu_2Ga_5$-type structure [18]. Herein we report its synthesis and structure and bonding along with various physical properties including magnetization, specific heat, and electrical resistivity.

2. Experimental

2.1. Synthesis

The starting materials—Ce (pieces, > 99.9%, Ames Laboratory), Pd, and Al (shot, > 99.99%, Alfa) were used as received. The reactions were carried out in 2 cm^3 alumina crucibles that were sealed in fused silica ampoules under vacuum. The elements were loaded according to the stoichiometric ratio of Ce:Pd:Al (1:2:20)

* Corresponding author at: Materials Physics and Application Division, MPA-10, Los Alamos National Laboratory, Los Alamos, NM 87545, USA. Fax: +1 505 665 7652.
E-mail address: ptobash@lanl.gov (P.H. Tobash).

0022-4596/$ - see front matter Published by Elsevier Inc.
doi:10.1016/j.jssc.2009.12.010

with the excess of Al to act as a metal flux. The reaction vessel was heated to 1000 °C (rate ca. 160°/h) where it was then held for 5.2 h and subsequently slowly cooled to 700 °C (rate ca. 5.5°/h). The reaction was quickly removed from the furnace and the excess Al was removed through centrifugation. The crystals isolated from the reaction had a plate-like habit. Fortunately, the crystals were large enough (2–4 mm in diameter) so that one crystal could be used for all of the measurements which was also beneficial for sorting out the anisotropy evidenced through the subsequent magnetization measurements (discussed below).

2.2. Powder X-ray diffraction

X-ray powder diffraction patterns were taken at room temperature on a Scintag powder diffractometer using monochromated Cu$K\alpha$ radiation. The typical scans included $\theta-\theta$ runs ($2\theta_{max}$=80°) with intervals of 0.02° and a 10 s counting time. The data analysis was carried out using the JADE 6.5 software package [19]. The samples were prepared by taking the plate-like crystals and grinding to a fine powder. There was good agreement with the positions and the intensities of the experimentally observed peaks and those calculated from the crystal structure.

2.3. Single-crystal X-ray diffraction

Single-crystal data collections on the flux-grown crystals were done on a Bruker CCD diffractometer. The crystals were cut to suitable dimensions (approximately 60 μm in all directions) and mounted onto a glass fiber on the goniometer using Paratone-N oil. Single-crystal data were collected at 120 K in four batch runs at different ω and φ angles. The SMART [20] and SAINT [21] programs were used for the data collection, integration, and refinements. SADABS [22] was used for semi-empirical absorption correction based on equivalents. The SHELX-package [23] was used to solve the structure by direct methods and also for the refinement by full matrix least-squares methods on F^2. All of the sites were refined with anisotropic displacement parameters. Only the Al1 atom, located at Wyckoff site 2*h* was found to be a statistical mixture with Pd (Al:Pd 75:25). All other sites behaved normal when their site occupancies were free to vary. Further details of the data collection and parameters from the structure refinements are provided in Table 1. The atomic coordinates and interatomic distances are compiled in Tables 2 and 3. The corresponding crystallographic information file (CIF) has also been deposited with Fachinformationszentrum Karlsruhe, 76344 Eggenstein-Leopoldshafen, Germany (fax: +49 7247 808 666; e-mail: crysdata@fiz.karlsruhe.de)-depository number CSD-420861.

2.4. Magnetic susceptibility measurements

Field-cooled *dc* magnetization (M) measurements were performed on a Quantum Design MPMS SQUID magnetometer. The measurements were taken in the temperature range of 350–2 K and in an applied magnetic field (H) of 0.1 T. The raw magnetization data were corrected for the holder contribution and converted to molar susceptibility ($\chi_m=M/H$). Magnetization data as a function of applied field were also collected on one single crystal at a temperature of 2 K and up to fields of 6 T. For both measurements, the single plate was measured along both directions of the applied field.

2.5. Specific heat and resistivity measurements

The data for the specific heat and electrical resistivity measurements were collected on a Quantum Design PPMS system. The flux-grown crystals from the single-crystal X-ray diffraction experiments were used for the calorimetry measurements, which were performed via a thermal relaxation method down to 0.4 K and in magnetic fields up to 9 T. The resistance was measured using a four-probe technique from 300 to 2 K with an excitation current of 1 mA. The Pt wire contacts were attached to the polished face of the crystal by spot welding.

Table 1
Selected single-crystal data and structure refinement parameters for $CePd_{1.5}Al_{5.5}$.

Empirical formula	$CePd_{1.5(1)}Al_{5.5(1)}$
Formula weight	448.11 g/mol
Collection temperature	120 K
Radiation, wavelength (λ)	0.71073
Crystal system	Tetragonal
Space group	*P*4/*mmm*
Unit cell dimensions	a=4.2298(6) Å c=8.075(2) Å
Unit cell volume, Z	144.48(5) Å^3,1
Density (ρ_{calc})	5.150 g cm^{-1}
Absorption coefficient (μ)	13.081 mm^{-1}
Crystal size	0.070 × 0.055 × 0.032
Reflections collected, R_{int}	878, 0.0261
Unique reflections	130
Data/restraints/parameters	129/0/14
GOF on F^2	1.278
Final R indices[a] ($I>2\sigma_{(I)}$)	R_1=0.0207 wR_2=0.0458
Final R indices[a] (all data)	R_1=0.0208 wR_2=0.0459

[a] $R_1=\Sigma||F_o|-|F_c||/\Sigma|F_o|$; $wR_2=[\Sigma[w(F_o^2-F_c^2)^2]]^{1/2}$, and $=1/[\sigma^2F_o^2+(0.0272P)^2+0.00P]$, $P=(F_o^2+2F_c^2)/3$.

Table 2
Atomic coordinates and equivalent isotropic displacement parameters (U_{eq}[a]) for $CePd_{1.5}Al_{5.5}$.

Atom	Wyckoff site	x	y	z	U_{eq}
Ce	1*a*	0	0	0	0.0063(3)
Pd	1*b*	0	0	$\frac{1}{2}$	0.0058(3)
Al1[b]	2*h*	$\frac{1}{2}$	$\frac{1}{2}$	0.1476(2)	0.0051(4)
Al2	4*i*	0	$\frac{1}{2}$	0.3276(2)	0.0081(4)

[a] U_{eq} is defined as one-third of the trace of the orthogonalized U_{ij} tensor.
[b] Refined as a mixture of Al and Pd in a ratio 75:25.

Table 3
Selected bond distances (Å) in $CePd_{1.5}Al_{5.5x}$.

Ce	Al1 × 8	3.220(2) Å
	Al2 × 8	3.387(3) Å
Pd	Al2 × 8	2.5321(9) Å
Al1	Al1	2.384(3) Å
Al1	Al2 × 4	2.5662(12) Å
Al2	Al2	2.785(3) Å
Al2	Al2 × 4	2.9909(4) Å

3. Results and discussion

3.1. Synthesis, structure, and bonding

The $CePd_{1+x}Al_{6-x}$ compound (where x=0.5) crystallizes with the $SrAu_2Ga_5$-type structure [18] in the tetragonal space group *P*4/*mmm*. The refined single-crystal non-integer formula arises from a mixture of Pd and Al specifically on the 2*h* Wyckoff site in

the crystal structure. This is the position which caps the Al2 square lattice and subsequently composes (Pd/Al)Al_4 tetrahedra; similar behavior was found in the isostructural $LaNi_{1+x}Al_{6-x}$ in which the 2*h* site was also found to be a statistical mixture of Ni and Al [24].

The structure can be seen as the building up of face-sharing $CeAl_{16}$ polyhedra in addition to corner-shared $PdAl_8$ blocks stacked on top of one another along the crystallographic *c*-axis. As shown in Fig. 1, this sort of construction is reminiscent to the crystal chemistry found for the '115' family of compounds, the only difference being the way in which the square lattice of atoms (Al in $CePd_{1.5}Al_{5.5}$ and In in $CeRhIn_5$) are connected. As pictured, the In atoms share a common vertex of the square pyramid, resulting in Ce atoms with 12 nearest neighbors ($CeIn_3$ block). The Ce–Al distances in $CePd_{1.5}Al_{5.5}$ are of the order 3.2–3.4 Å, similar to those found in $CeAl_4$ [18], $Ce_4Ni_6Al_{23}$ [25], $Ce_2Al_3Ge_4$ [26], and CeAl [18]. The Pd–Al distance in the $PdAl_8$ blocks measure 2.53 Å which is similar with those found in $CePd_2A_3$ [18] and $CePdAl_3$ [27]. The Ce–Al distances are slightly smaller than the Ce–Ga distance in $CePdGa_6$ while the Pd–A1 distances are similar to the Pd–Ga distances within the Pd layers [15]. There is also a significant difference in the unit cell parameters between $CePd_{1.5}Al_{5.5}$ and $CePdGa_6$ [15], where the *a*-axis in $CePd_{1.5}Al_{5.5}$ shows nearly a 3% decrease (where a=4.350(3) Å in $CePdGa_6$ and 4.2298(6) Å in $CePd_{1.5}Al_{5.5}$) and the *c*-axis shows a 2% increase (c=7.922(6) Å in $CePdGa_6$ and 8.075(2) Å in $CePd_{1.5}Al_{5.5}$). This could have an influence for the overall magnetic behavior between both compounds as discussed below.

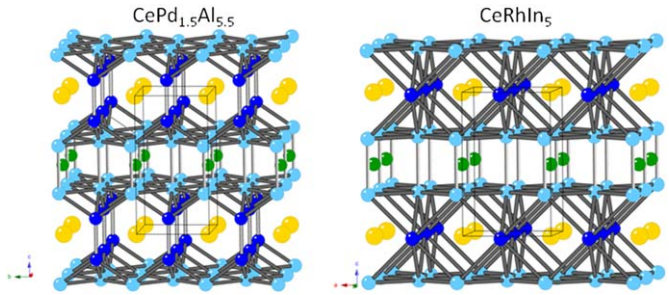

Fig. 1. Crystal structure of $CePd_{1.5}Al_{5.5}$ viewed approximately down the crystallographic *a*-axis and emphasizing the Ce polyhedra formed with the Al atoms. The structure is closely related to that of $CeRhIn_5$. The unit cells are drawn for both structures with the Ce, Pd(Rh), and Al(In) atoms being represented with yellow, green, and blue [Al1(In1) dark blue and Al2(In2) light blue] colors, respectively (color for web version only).

3.2. Magnetic susceptibility

Fig. 2 shows the magnetic susceptibility $\chi(T)$ collected on a single-crystal in the temperature range between 2 and 350 K in an applied field of 0.1 T in which the field was aligned along the *ab* crystallographic plane and along the *c*-axis. The $\chi=M/H$ plot as a function of temperature reveals Curie–Weiss behavior above 200 K for both field directions. Fits of the data to $\chi(T)=C/(T-\theta_{CW})$, where $C=N_A\mu_{eff}^2/3k_B$ is the Curie constant and θ_{CW} is the Curie–Weiss temperature, yields an effective moment of $2.18\mu_B$ normalized per Ce atom for $H||ab$, which is somewhat lower than the expected Ce^{3+} magnetic moment resulting in a value of $2.54\mu_B$ [28]. The Curie–Weiss temperature, θ_{CW} is 19.6 K for $H||ab$, indicating the presence of ferromagnetic correlations within the *ab* plane, while strong antiferromagnetic correlations are present along the *c*-axis. This is suggested from the large negative Curie–Weiss temperature $\theta_{CW}=-144$ K determined from the $\chi^{-1}(T)$ data with an effective moment of $2.59\mu_B$ per Ce atom. Taking both directions of the crystal into account, a polycrystalline average for $\mu_{eff(poly)}=\frac{2}{3}\chi_a+\frac{1}{3}\chi_c$ results in a value of $2.32\mu_B$. The magnified view of the low temperature $\chi(T)$ data below 15 K in inset (A) in Fig. 2 emphasizes the difference between both orientations where the data corresponding to when the field is parallel to the *ab* plane is nearing ferromagnetic ordering around 3 K. With this observed anisotropy, it can be suggested that the easy axis of magnetization

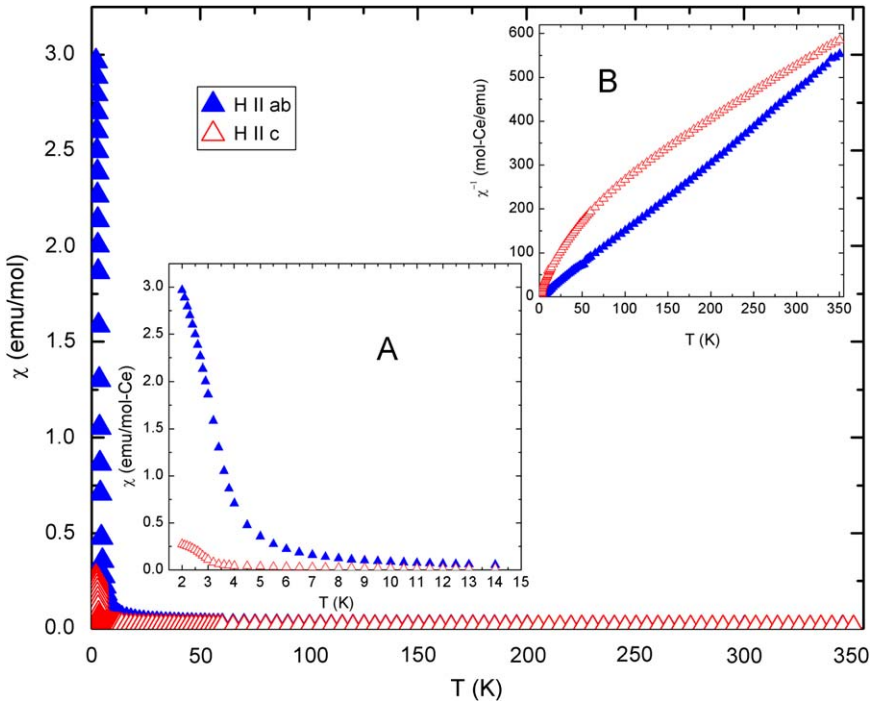

Fig. 2. Temperature dependence of the magnetic susceptibility (χ) of $CePd_{1.5}Al_{5.5}$ measured in a magnetic field of 0.1 T along both directions of the tetragonal crystal. Inset (A): χ vs. *T* below 15 K. Inset (B): Inverse magnetic susceptibility $\chi^{-1}(T)$.

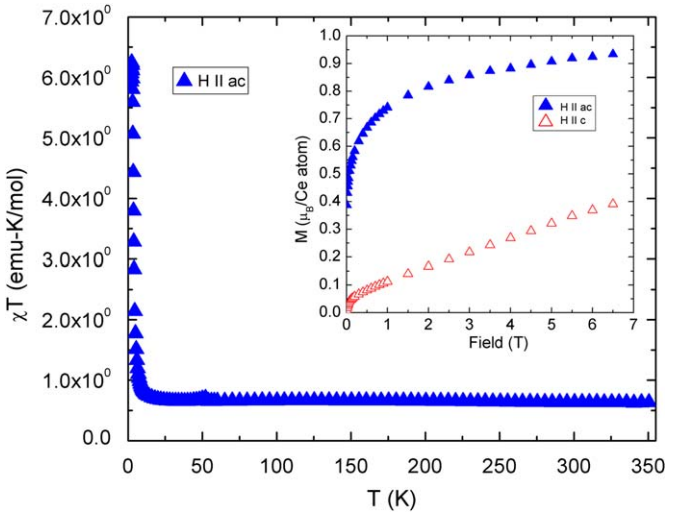

Fig. 3. $\chi(T)$ as a function of temperature emphasizing the sharp increase at lower temperatures. Magnetization (M) vs. applied field (H) for $CePd_{1.5}Al_{5.5}$ measured at 2 K up to a field of 6 T is shown in the inset for both directions of the single crystal.

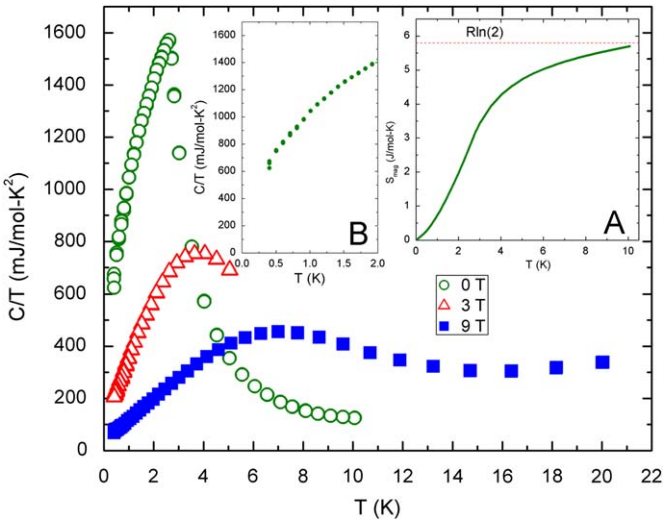

Fig. 4. Specific heat plotted as C/T vs. T, of $CePd_{1.5}Al_{5.5}$ in magnetic fields up to 9 T with applied field parallel to the *ab* plane. Inset (A): The magnetic entropy $S_{mag}(T)$ of $CePd_{1.5}Al_{5.5}$. Inset (B): Zoomed in view of heat capacity data below 2 K.

resides in the crystallographic *ab* plane while the hard axis lies along the crystallographic *c*-axis. Also noteworthy is the possibility for the presence of strong crystal field effects that are most apparent when the applied magnetic field is aligned parallel to the *c*-axis as evident from the large curvature from the $\chi^{-1}(T)$ data shown within inset (B) in Fig. 2. As provided in Fig. 3, below 5 K, further confirmation of the ferromagnetic phase transition is evident by $\chi(T)$ increasing rapidly with decreasing temperature signaling the onset of ferromagnetism in $CePd_{1.5}Al_{5.5}$. The magnetization M vs. H in the inset of Fig. 3 shows both the spontaneous magnetization and the saturation magnetization at 2 K for both field orientations. As related to the differences in the magnetization data in Fig. 2, the same model for the magnetic moments on the Ce atoms can be applied—the easy axis of magnetization is in the *ab* plane where the Ce moments are collinear and coupled ferromagnetically, while the hard axis is along the *c*-axis and under an applied magnetic field these moments cannot be ferromagnetically coupled but instead are canted out of the *ab* plane. Of course in order to support this hypothesis for the magnetic sublattice neutron diffraction experiments would need to be completed and further more detailed studies are currently underway. A fit of the $M(H)$ data above 5 T for $H||ab$ yields $M_{sat}=1.0\mu_B$/Ce atom, consistent with a localized Ce^{3+} ferromagnetic state (the expected magnetic moment is $\mu_{ord}=gJ\,\mu_B=6/7\times5/2\mu_B=2.14\mu_B$ which is calculated in the absence of crystal field effects but if these are taken into account with a Ce^{3+} in a ground state doublet this value is $1.24\mu_B$ which is indeed much closer to the saturated value in M vs. H).

It is noteworthy that the magnetization of $CePd_{1.5}Al_{5.5}$ is much different to that observed for $CePdGa_6$ where a sharp increase in $M(H)$ at 2 T suggests metamagnetic behavior [15]. Furthermore, while $CePd_{1.5}Al_{5.5}$ orders ferromagnetically, $CePdGa_6$ is an antiferromagnet in which the Ce moments likely point along the crystallographic *c*-axis; these different types of magnetic order could arise from the small increase in the *c* lattice parameter in $CePd_{1.5}Al_{5.5}$ compared to that in $CePdGa_6$ through, i.e., a modification of the RKKY exchange constant and/or different hybridization of the Ce–Al and Ce–Ga bonding contacts. Another possibility for the observed differences is the crystallographic disorder which exists in $CePd_{1.5}Al_{5.5}$ when compared to the stoichiometric $CePdGa_6$ [15].

3.3. Specific heat

The specific heat of $CePd_{1.5}Al_{5.5}$, plotted as $C_p(T)/T$ vs. T is shown in Fig. 4 at various magnetic fields up to 9 T in fields parallel to the *ab* crystallographic plane. A λ-type anomaly is observed with a peak in $C_p(T)/T$ at around a temperature of $T_C=2.8$ K in zero field. Upon application of a magnetic field, as shown in Fig. 4, this anomaly broadens and moves up in temperature in fields of 3 and 9 T, which is typical for a ferromagnetically ordered system. As shown in the inset (A) of Fig. 4, the magnetic entropy of $CePd_{1.5}Al_{5.5}$ determined by the total area under the zero field $C_p(T)/T$ curve assuming no phonon contribution to the specific heat up to 10 K. Unfortunately a La analog could not be synthesized in order to precisely determine the magnetic contribution to the specific heat. Using the previous method to obtain the magnetic contribution to the specific heat, the magnetic entropy $S_{mag}=\Sigma(C/T)\,dT$ at the ordering temperature $T_C=2.8$ K, is only about one-half $R\ln(2)$, but by 10 K, the full entropy $R\ln(2)$ expected for a doublet ground state of Ce^{3+} in the tetragonal crystalline electric field is recovered. As provided in inset (B), the Sommerfeld coefficient γ extracted from the $C_p(T)/T$ data for $CePd_{1.5}Al_{5.5}$ in the ordered state is $\sim$500 mJ/mol-K^2 which was determined by the resulting intercept from a linear fit below the ordering temperature from the zero field data. Such a large specific heat coefficient in a Ce-containing compound in the ordered state is rare but has also been observed for several U compounds such as UCd_{11} [29], U_2Zn_{17} [30], and UIr_2Zn_{20} [31].

3.4. Electrical resistivity

The $\rho(T)$ data of $CePd_{1.5}Al_{5.5}$ shown in Fig. 5 displays a gradual decrease in the resistivity with decreasing temperature. As can be seen within the inset of Fig. 5, the downturn below 5 K is indicative of the ferromagnetic ordering as evidenced from the specific heat measurements. The residual resistivity ratio RRR=1.5 is most probably an artifact of the crystallographic disorder. The small minimum in $\rho(T)$ may be due to the depopulation of an excited crystal field level with decreasing temperature and has also been observed in compounds such as $CeNiSb_3$ [32,33] and $CeSn_{0.7}Sb_2$ [34]. From $\rho(T)$ of $YbBe_{13}$, which also shows similar behavior, has been suggested to arise from "Kondo sideband"

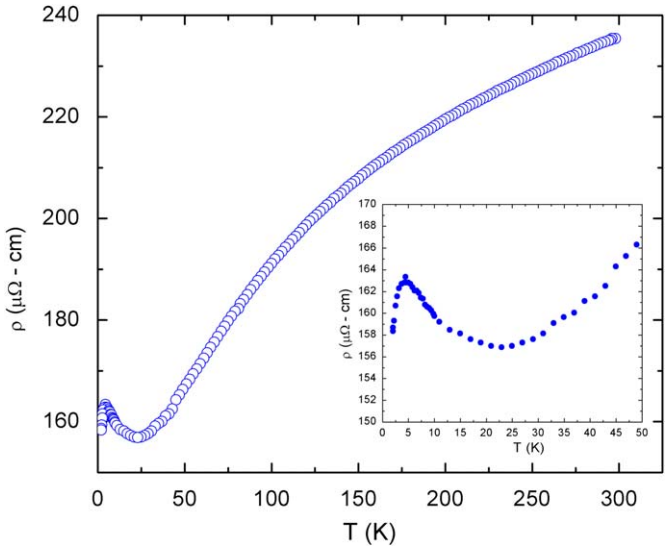

Fig. 5. Electrical resistivity $\rho(T)$ of $CePd_{1.5}Al_{5.5}$ from 2 to 300 K. Inset shows $\rho(T)$ below 50 K.

scattering [35]. No evidence for superconductivity was observed down to 0.4 K.

4. Conclusion

A new compound, $CePd_{1.5}Al_{5.5}$, has been synthesized using in Al flux. The compound crystallizes with the $SrAu_2Ga_5$ structure type in the tetragonal space group $P4/mmm$. The magnetic susceptibility, specific heat, and electrical resistivity reveals that it undergoes ferromagnetic ordering at T_C=2.8 K in the absence of an applied magnetic field. The magnetization measured along both directions of the crystal show that the easy axis of magnetization is along the *ab* crystallographic plane which suggests that the Ce magnetic moments lie in the plane, while the moments along the crystallographic *c*-axis are non-collinear or canted when a magnetic field is applied.

Acknowledgments

Paul H. Tobash acknowledges financial support from Los Alamos National Laboratory through the Seaborg Fellowship. Work at Los Alamos was performed under the auspices of the US DOE and is also funded in part by the Los Alamos Laboratory Directed Research and Development program. Work at University of Delaware was supported by a NSF CAREER grant (DMR-0743916).

Appendix A. Supplementary material

Supplementary data associated with this article can be found in the online version at doi:10.1016/j.jssc.2009.12.010.

References

[1] G.R. Stewart, Rev. Mod. Phys. 56 (1984) 755.
[2] H.v. Löhneysen, T. Pietrus, G. Portisch, H.G. Schlager, A. Schröder, M. Sieck, T. Trappmann, Phys. Rev. Lett. 72 (1994) 3262.
[3] J.D. Thompson, R. Movshovich, Z. Fisk, F. Bouquet, N.J. Curro, R.A. Fisher, P.C. Hammel, H. Hegger, M.F. Hundley, M. Jaime, P.G. Pagliuso, C. Petrovic, N.E. Phillips, J.L. Sarrao, J. Magn. Magn. Mater. 226 (2001) 5.
[4] F. Steglich, J. Aarts, C.D. Bredl, W. Lieke, D. Meschede, W. Franz, H. Schafer, Phys. Rev. Lett. 43 (1979) 1892.
[5] C. Petrovic, P.G. Pagliuso, M.F. Hundley, R. Movshovich, J.L. Sarrao, J.D. Thompson, Z. Fisk, P. Monthoux, J. Phys.: Condens. Matter 13 (2001) L337.
[6] E. Bauer, G. Hilscher, H. Michor, C. Paul, E.W. Scheidt, A. Gribanov, Y. Seropegin, H. Noel, M. Sigrist, P. Rogl, Phys. Rev. Lett. 92 (2004) 027003.
[7] J.M. Lawrence, J.D. Thompson, Y.Y. Chen, Phys. Rev. Lett. 54 (1985) 2537.
[8] R.A. Gordon, Y. Ijiri, C.M. Spencer, F.J. Disalvo, J. Alloys Compd. 224 (1995) 101.
[9] M.F. Hundley, P.C. Canfield, J.D. Thompson, Z. Fisk, J.M. Lawrence, Phys. Rev. B 42 (1990) 6842.
[10] H. Hegger, C. Petrovic, E.G. Moshopoulou, M.F. Hundley, J.L. Sarrao, Z. Fisk, J.D. Thompson, Phys. Rev. Lett. 84 (2000) 4986.
[11] E.G. Moshopoulou, Z. Fisk, J.L. Sarrao, J.D. Thompson, J. Solid State Electrochem. 158 (2001) 25.
[12] Ya.M. Kal'ichak, V.I. Zaremba, V.M. Baranyak, V.A. Bruskov, P.Yu. Zavalii, Izv. Akad. Nauk 1989 (1989) 213.
[13] E.G. Moshopoulou, R.M. Ibberson, J.L. Sarrao, J.D. Thompson, Z. Fisk, Acta Crystallogr. B 62 (2006) 173.
[14] R.T. Macaluso, J.L. Sarrao, N.O. Moreno, P.G. Pagliuso, J.D. Thompson, F.R. Fronczek, M.F. Hundley, A. Malinowski, J.Y. Chan, Chem. Mater. 15 (2003) 1394.
[15] R.T. Macaluso, S. Nakatsuji, H. Lee, Z. Fisk, M. Moldovan, D.P. Young, J.Y. Chan, J. Solid State Chem. 174 (2003) 296.
[16] R.T. Macaluso, J.N. Millican, S. Nakatsuji, H. Lee, B. Carter, N.O. Moreno, Z. Fisk, J.Y. Chan, J. Solid State Chem. 178 (2005) 3547.
[17] D. Kaczorowski, A.P. Pikul, D. Gnida, V.H. Tran, Phys. Rev. Lett. 103 (2009) 027003.
[18] P. Villars, L.D. Calvert, Pearson's Handbook of Crystallographic Data for Intermetallic Phases, 2nd ed, American Society for Metals, Materials Park, OH, 1991.
[19] JADE Version 6.5, Materials Data, Inc., Livermore, CA, 2003.
[20] SMART NT, Version 5.63, Bruker Analytical X-ray Systems, Inc., Madison, WI, 2003.
[21] SAINT NT, Version 6.45, Bruker Analytical X-ray Systems, Inc., Madison, WI, 2003.
[22] SADABS NT, Version 2.10, Bruker Analytical X-ray Systems, Inc., Madison, WI, 2001.
[23] SHELXTL, Version 6.12, Bruker Analytical X-ray Systems, Inc., Madison, WI, 2001.
[24] D. Gout, E. Benbow, O. Gourdon, G.J. Miller, Inorg. Chem. 43 (2004) 4604.
[25] D. Gout, E. Benbow, O. Gourdon, G.J. Miller, J. Solid State Chem. 174 (2003) 471.
[26] H. Flandorfer, D. Kaczorowski, J. Groebner, P. Rogl, R. Wouters, C. Godart, A. Kostikas, J. Solid State Chem. 137 (1998) 191.
[27] C. Schank, F. Jahrling, L. Luo, A. Grauel, C. Wassilew, R. Borth, G. Olesch, C.D. Bredl, C. Geibel, F. Steglich, J. Alloys Compd. 207 (1994) 329.
[28] J.S. Smart, Effective Field Theories of Magnetism, Saunders, Philadelphia, PA, 1966.
[29] Z. Fisk, G.R. Stewart, J.O. Willis, H.R. Ott, F. Hulliger, Phys. Rev. B 30 (1984) 6360.
[30] H.R. Ott, H. Rudigier, P. Delsing, Z. Fisk, Phys. Rev. Lett. 52 (1984) 1551.
[31] E.D. Bauer, A.D. Christianson, J.S. Gardner, V.A. Sidorov, J.D. Thompson, J.L. Sarrao, M.F. Hundley, Phys. Rev. B 74 (2006) 155118.
[32] R.T. Macaluso, D.M. Wells, R.E. Sykora, T.E. Albrecht-Schmitt, A. Mar, S. Nakatsuji, H. Lee, Z. Fisk, J.Y. Chan, J. Solid State Chem. 177 (2004) 293.
[33] V.A. Sidorov, E.D. Bauer, H. Lee, S. Nakatsuji, J.D. Thompson, Z. Fisk, Phys. Rev. B 71 (2005) 094422.
[34] L. Deakin, M.J. Ferguson, M.J. Sprague, A. Mar, R.D. Sharma, C.H.W. Jones, J. Solid State Chem. 164 (2002) 292.
[35] J.D. Thompson, Z. Fisk, J.O. Willis, in: U. Eckern, A. Schmid, W. Weber, H. Wühl (Eds.), Proceedings of the 17th International Conference of Low Temperature Physics, North-Holland, Amsterdam, 1984, p. 323.